

# HYDRAULICS OF DOUBLE STILLING BASIN SYSTEMS

László HAYDE

Department of Hydraulic Engineering  
Budapest University of Technology and Economics  
H–1521 Budapest, Hungary

Received: April 20, 2000

## Abstract

Practical application of broken-axis stilling basin systems can provide significant financial benefits. At this moment there is no generally accepted calculation method for their design. Based on physical model investigations an approximate theoretical model has been developed. This model makes it possible to describe the hydraulic phenomena proceeding in the double, broken-axis stilling basin systems.

Main elements of the theoretical model:

- 1<sup>st</sup> part of the upper basin, dimensioned on the basis of throwing distance of free jet.
- 2<sup>nd</sup> part of the upper basin, calculated by impulse-momentum theorem.
- 3<sup>rd</sup> part of the upper basin, the lateral weir, for whose calculation a new method has been developed.

During the physical model investigation of the lateral weir it has been proved that for a suitable velocity distribution in the lower basin a relatively homogeneous discharge distribution is required along the lateral weir. This can be attained by a linearly changing height of the weir. No research is required in the lower basin if the influx from the weir has a uniform distribution.

The practical applicability of the complex theoretical description adjusted to the different phenomena was checked by the results on the double stilling basin with axis broken by  $90^\circ$ . This comparison has proved the practical applicability of the theoretical formulas.

*Keywords:* hydraulic engineering structure, energy dissipation, stilling basin, spillway system, physical model investigation, theoretical model, broken-axis stilling basin systems.

## 1. Introduction

Hydraulic model investigations of the structures of the Duhok reservoir (Iraq) were carried out at the Department of Hydraulic Engineering of the Technical University of Budapest between January 1981 and January 1982, by Professor Ottó Haszpra and his staff.

For the final forming of the double stilling basin connecting to the morning glory spillway system (funnel, shaft, diversion tunnel) a new solution was proposed with excentric inflow to the upper basin and nearly homogeneous overflow to the lower basin over a special lateral weir. (HASZPRA [2])

Briefly summarising the main characteristics of this unique solution the most important fact to be emphasised is the energy dissipation of the water jet flowing out

of the tunnel combined with the change of flow direction. The angle between the entrance direction of the inflow jet and the outflow current direction to the river-bed is  $78^{\circ}40'$ . The most important consequence of the proposed solution was that the 7 m diameter tunnel of the spillway system to be built in rock could have been 200 m shorter allowing significant financial savings. Nevertheless, the broken-axis stilling basin system can make the required energy dissipation and the nearly homogeneous velocity distribution necessary for the diversion to the natural riverbed.

After successfully completing this concrete research, based on the interest manifested on domestic and international conferences, generalising investigations have been started (HASZPRA [1]; HAYDE [6]; PAPP [11]) to find the different forming of the double stilling basin systems for different breaking angles between  $0^{\circ}$  and  $90^{\circ}$ . These investigations have also successfully proved the satiability of the requirements for the whole range of breaking angles.

Between 1993 and 1997 the National Scientific Research Fund has financed the research work headed by Professor Haszpra for the theoretical and mathematical mapping of the phenomena. The results briefly described in this paper were presented in the 'dr. univ.' thesis of the author in detailed form (HAYDE [7]).

## 2. Hydraulic Model Tests of the Broken-Axis Stilling Basin System of the Duhok Dam

The location of the structures of the spillway system is shown in *Fig. 1*. The numbers stand for the following structures:

1. dam
2. morning glory spillway and shaft
3. diversion tunnel and bottom outlet
4. stilling basin system
5. alternative for the diversion tunnel if a straight-axis stilling basin is needed.

(It can be seen that the diversion tunnel can be almost 200 meters shorter provided that the broken-axis stilling basin can make the required dissipation. Considering the facts that the diameter of the diversion tunnel is 7 m and it goes in rock this stilling basin system could result in savings in capital investments.)

The first basic variant of the broken-axis stilling basin system was designed by Vodproject (Bulgaria) for the 1/1000 probability flood, with a maximum discharge of  $480 \text{ m}^3/\text{s}$ . It is shown in *Fig. 2*. This variant was investigated in a 1:50 scale hydraulic model. The exit velocity distribution, from the lower basin above its sill is given in *Fig. 2*. It can be seen that in this variant the exit velocity varied between 9 m/s and  $-3 \text{ m/s}$  along the cross section which obviously cannot be allowed for the river-bed.

The design case for the second basic variant of the spillway system and the stilling basin system was the 1/10000 probability flood with a maximum discharge of  $810 \text{ m}^3/\text{s}$  (after having considered the retentive effect of the reservoir as well)

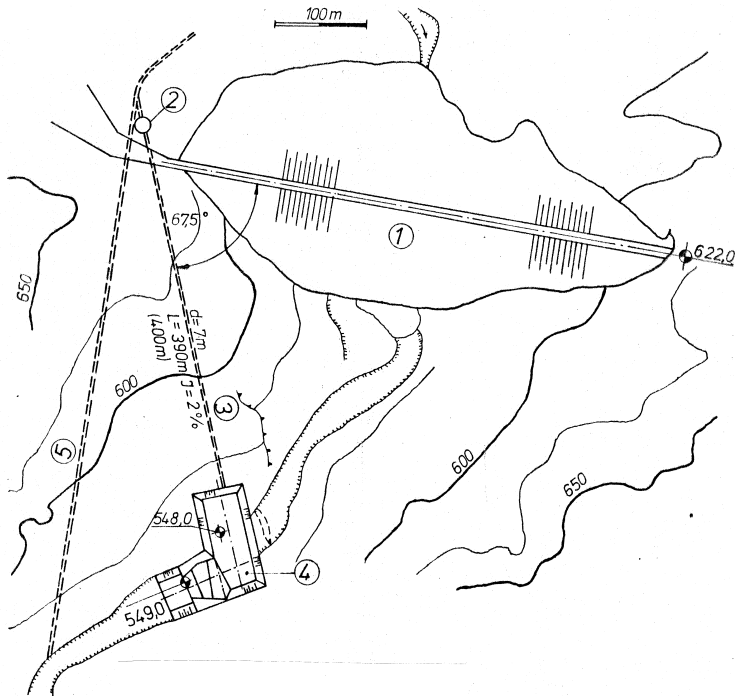


Fig. 1. Location of the structures of the spillway system

because there is an inhabited area (the city of Duhok) downstream the structure in a 1 km distance. The designer of this variant was the International Board of Experts (IBE) commissioned by the Ministry of Irrigation of Iraq. This suggested variant was studied in a 1:140 informative scale model. This variant was not satisfactory either, because the velocities measured in the exit section of the lower basin were between 0 m/s and 6 m/s. In this last model several variants of the stilling basin system were studied.

The location and the crest slope of the lateral weir between the upper and the lower basins were investigated first. The vertical and the horizontal position of the tunnel exit relative to the axis of the upper basin and the length of the upper basin were also investigated in the 1:140 informative scale model. The best variant of these series was used as the starting variant in the 1:50 scale model of the stilling basin system in which the details of the structures were elaborated.

All these tests led to the variant proposed to the Iraqi partner by the Department of Hydraulic Engineering of the Technical University of Budapest. This is illustrated in Fig. 3 and in Picture 1. The efficiency of this system is very good (Picture 2), for the whole discharge regime between 0 and 810 m<sup>3</sup>/s the exit velocity distribution is satisfactorily homogeneous (Fig. 4).

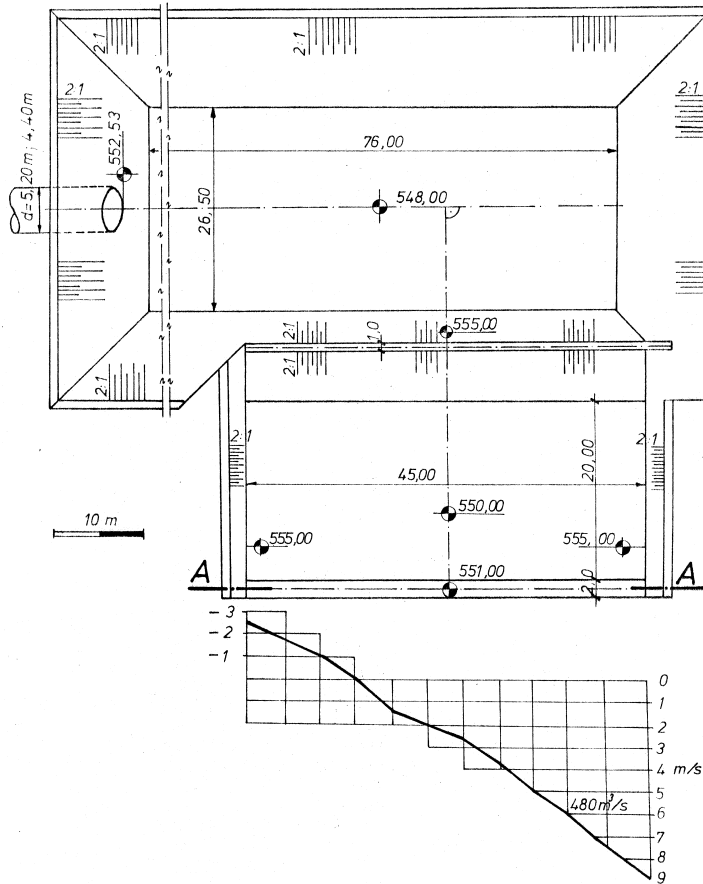


Fig. 2. Originally planned variant of the stilling basin system

The bottom of the upper basin is 100 m long (as it was suggested by the IBE). The vertical position of the tunnel exit was not changed either, but its horizontal position relative to the axis of the upper basin has to be at a distance of 7 m to the left side.

The slope and the elevation of the crest of the lateral weir between the upper and the lower basin can be seen in Section 2-2, while the profile of the weir is shown in Section 3-3 of Fig. 3.

In the part, critical from point of view of cavitation, of the upper basin detailed velocity and pressure distribution measurements were carried out. The piezometric taps can be seen in Picture 1. The results of the measurements are shown in Fig. 4. In this critical part of the basin, in order to avoid cavitation erosion of the bottom, at certain zones the permitted maximum values of the absolute roughness are  $\varepsilon = 0.15$

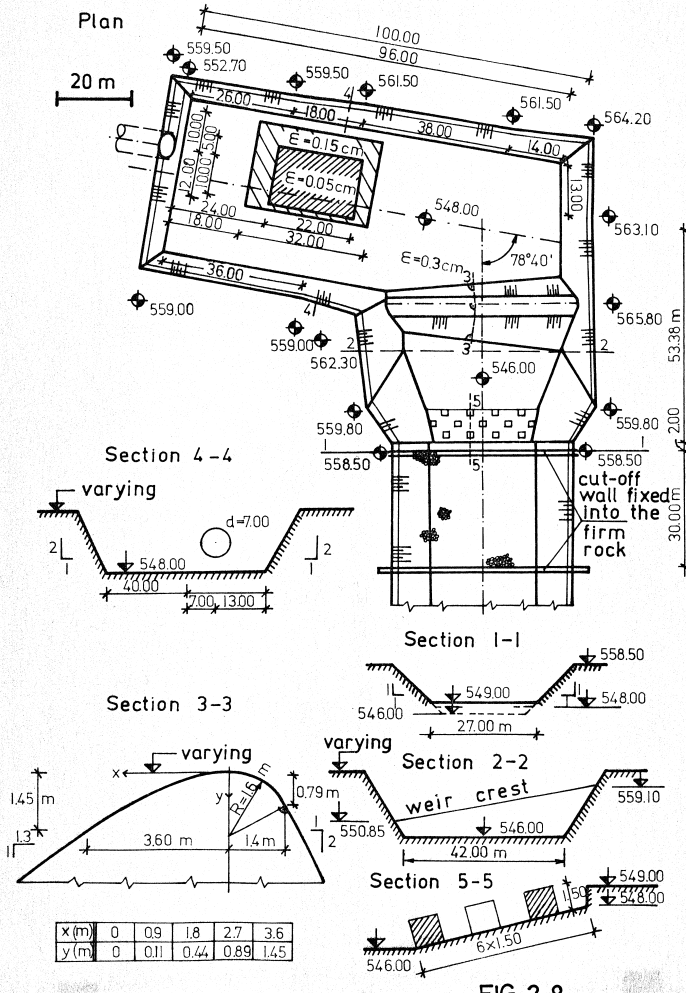


Fig. 3. Proposed variant of the stilling basin system

and 0.05 cm. These zones can be seen in Fig. 3. In the other parts of the basin an absolute roughness as high as  $\epsilon = 0.3$  cm is permitted.

In the lower basin cube-form block dissipators are built in, in order to make the exit velocity distribution more uniform. To ensure a satisfactory hydraulic jump and also to avoid cavitation erosion of the first blocks near to the downstream foot of the weir, a 4 meter deepening of the bottom level of the lower basin was needed. The arrangement of the block dissipators can be seen in the Plan and in the Section 5-5 of Fig. 3.

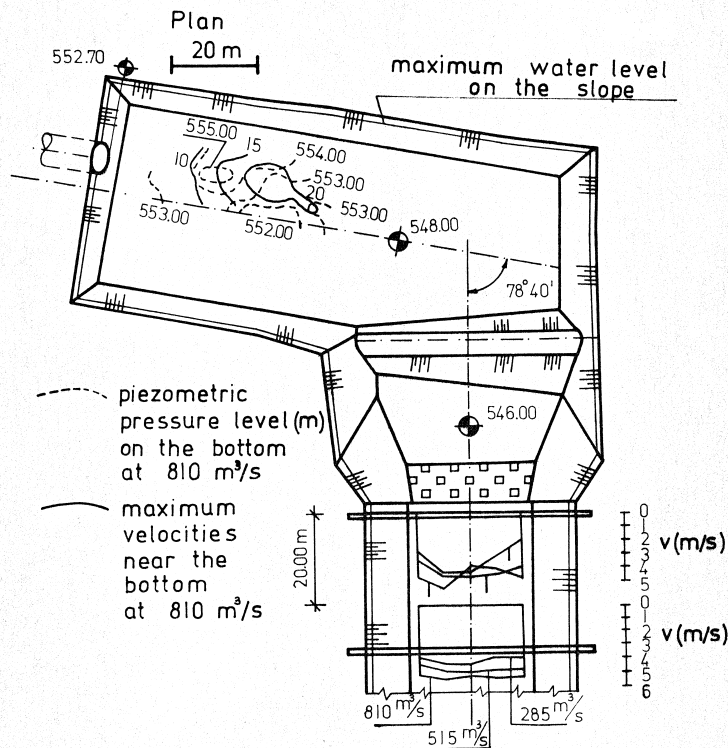


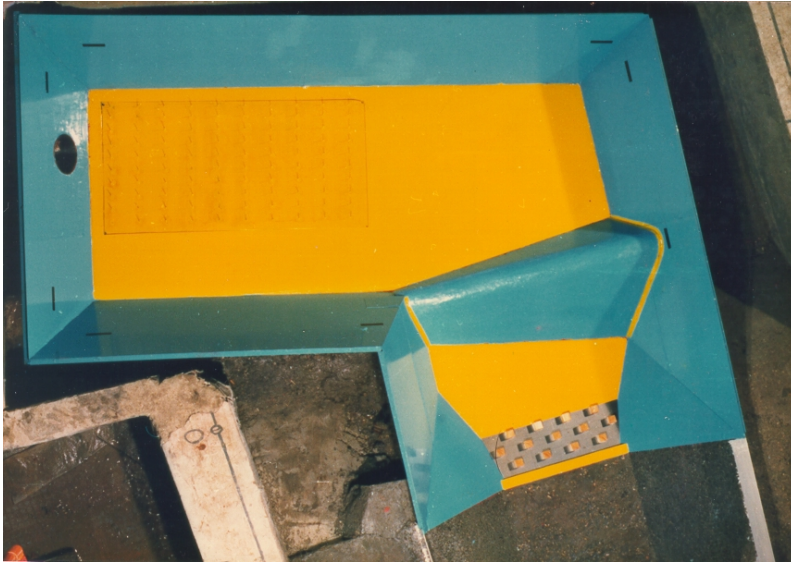
Fig. 4. Measured data of the proposed stilling basin system

The form of the lower basin is similar to a confusor, on the one hand to approximate the cross sectional form of the natural river bed and on the other hand to attain a practically homogeneous exit velocity distribution. By this arrangement of the lower basin the hydraulic jump was pressed back to the downstream slope of the weir.

After the sill (Section 1-1) of the lower basin, stone pitching was proposed by the designer. This is really needed but at the same time it is necessary too, to close both the sill and the downstream end of the stone pitching by firm cut-off walls fixed into the firm rock, downward and laterally, to avoid undermining the structure.

### 3. Generalising Model Tests for Investigating the Effects of the Breaking Angle ( $0^\circ$ – $90^\circ$ )

After the successful completion of the above detailed concrete research work, considering the fact that certain local and topographic conditions may require the application of broken-axis stilling basin systems in many other cases, generalising



*Picture 1.* Proposed variant of the stilling basin system in 1:50 scale model



*Picture 2.* Proposed variant of the stilling basin system in 1:50 scale model with the design discharge of  $810 \text{ m}^3/\text{s}$

investigations have been started to find the different forming of the double stilling basin systems for different breaking angles between  $0^\circ$  and  $90^\circ$ .

For these tests a vertical wall basin system was constructed which could be considered as a simplified model of the Duhok stilling basin system in scale 1:140. Just like the models of the structures of the Duhok dam this model was also operated according to the Froude law.

The measurements were performed for three discharges, which are marked in the diagram.  $810 \text{ m}^3/\text{s}$  for the 1/10000 probability flood;  $552 \text{ m}^3/\text{s}$  approximately for the 1/1000 probability flood and  $297 \text{ m}^3/\text{s}$  approximately for the 1/100 probability flood determined for the Duhok spillway. It must be mentioned that for generalisation it would have been better to give the results of the tests in non-dimensional forms but an easier comparison of the results with those obtained for the Duhok dam could be done this way.

The arrangements of the model with different breaking angles in  $22.5^\circ$  steps ( $90^\circ$ ,  $67.5^\circ$ ,  $45^\circ$ ,  $22.5^\circ$ , and  $0^\circ$ ) are very similar to each other, thus only one, the  $67.5^\circ$  model is presented in *Fig. 5*.

The varying data of the stilling basin system are marked with the following symbols:

$L$  : length of the upper basin

$Z$  : excentricity of the tunnel exit (the horizontal distance between the axis of the upper basin and that of the tunnel)

$X$  : horizontal distance between the weir crest and the sill in the lower basin.

The width of the upper and the lower basin was permanent.

After the investigation of several variants the comparison of the varying data of the best variants for each breaking angle are summarised in *Fig. 6*. The main parameters of the model are plotted against the breaking angle  $\alpha$ .

It can be stated that  $L$  and  $X$  does not depend on  $\alpha$  if the average height of the weir crest is always 6.25 m. If it is lower (as it was in the straight axis model) they are also varying. The relationships between  $\alpha$  on one hand and  $Z$ ,  $\beta$ , and  $b$  on the other hand ( $\beta$  is the elevation angle of the crest slope,  $b$  is the height of the weir at the higher end) also can be seen in *Fig. 6*.

Finally, it can be concluded that the form of the velocity distribution in the cross section of the lower basin does not depend perceivably on the breaking angle of the stilling basin system. The efficacy of the different angle best variants, from the point of view of energy dissipation, can be considered equal.

Considering the fact that in our model the widths of the basins were permanent, the study of the footing area of the structure is limited to the length of the basins. As it was mentioned before, the necessary length for the upper basin (not considering a slight deviation for the straight axis variant) proved to be permanent. As for the needed length of the lower basin an important, though only a comparative statement can be concluded:

Since there is not any significant deviation between the velocity distributions in the same sections of the different angle variants (or at least demonstrating a

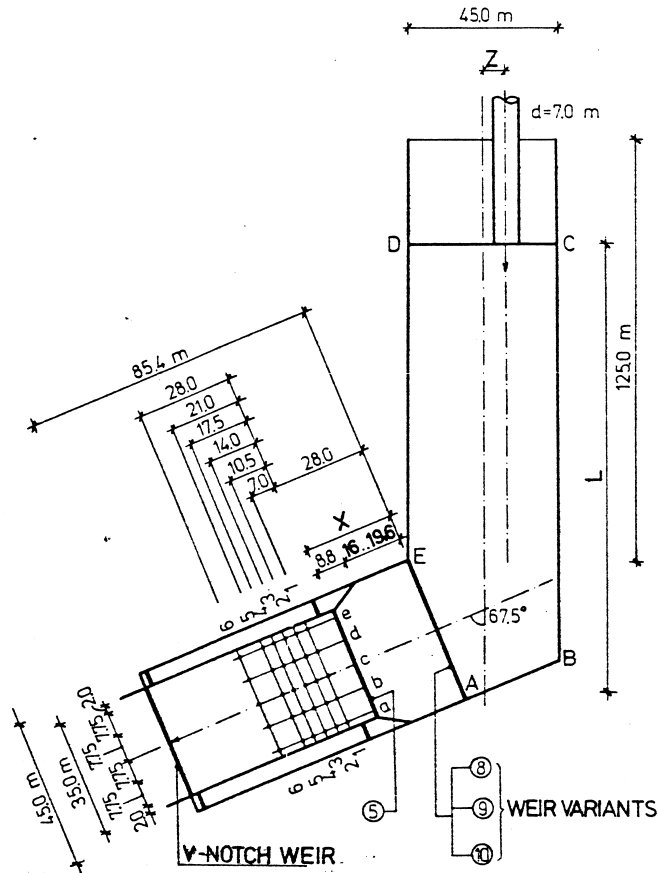


Fig. 5. Generalising model

reliable difference much more detailed measurement series with higher level instrumentation would be needed) it is rather obvious, that for the necessary length of the lower basin, too, no significant differences could be determined as depending on the breaking angle.

It means that for the same water jet a stilling basin system of the same footing area will work well, and changing the breaking angle does not result in any considerable economical consequences.

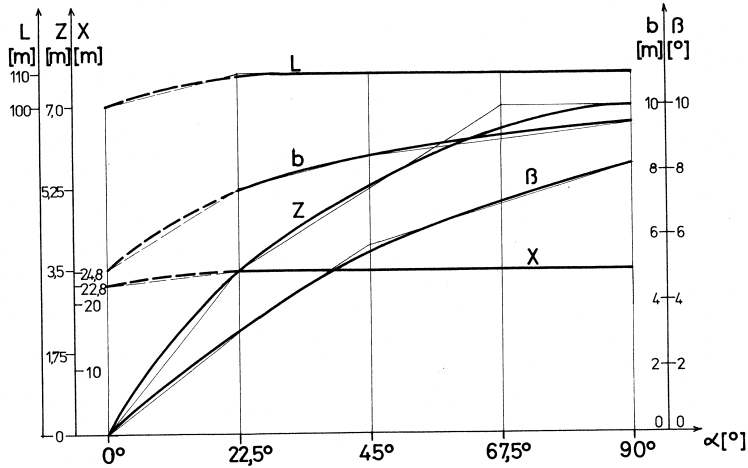


Fig. 6. Main parameters of the generalising model

#### 4. Theoretical Model of Double Stilling Basin Systems

The above detailed measurement results have proved that the special double stilling basin systems described can fulfil the requirements of energy dissipation and directional change at the same time. In this chapter an approximative theoretical model will be described developed for mapping the series of hydraulic phenomena proceeding in the double, broken-axis stilling basin systems.

The physical model investigations and the available literature have shown that the operation of these structures is built up from several different elements which have co-action and not even the individual elements have been completely solved or theoretically described. Thus, a rather new though simple theoretical model has been applied to describe the series of phenomena.

Comparing the calculation results of the theoretical model and the measurement results of the physical model investigations, the new theoretical model has shown adequate results. Elements and details of the theoretical model are described in Fig. 7.

##### 4.1. Elements of the Theoretical Model

The water jet enters the upper basin from a tunnel, which is, for the design case, a pressure conduit. At and after the entrance section, the water jet is surrounded by atmospheric pressure. After leaving the end of the tunnel the water jet has free fall, caused by gravity, into the upper basin. Taking the length of this horizontal casting it can be considered as the *first part of the upper basin*.

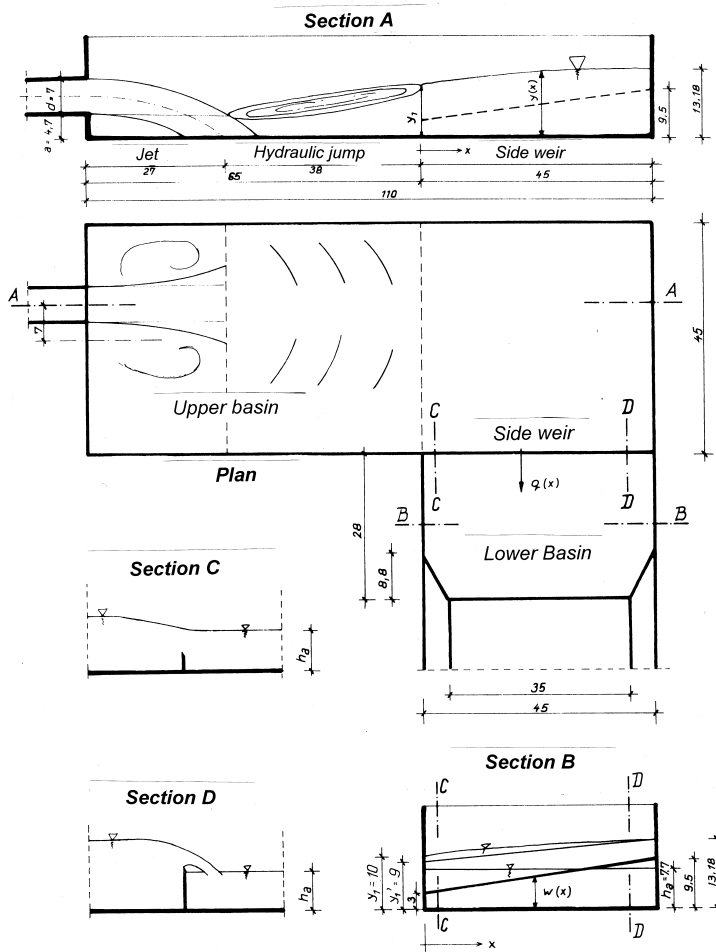


Fig. 7. Theoretical model of double stilling basin systems

From the entrance velocity  $v_t$  of the water jet (just leaving the tunnel) and the free fall velocity  $v_g$ , the resultant velocity  $v_1$  at or near the bottom of the upper basin can be determined.

$$v_1 = \sqrt{v_t^2 + v_g^2}.$$

Taking the path equation to the axis of the jet

$$Y_s = \frac{g}{2v_t^2} \cdot X_s^2.$$

$Y_s = a + r$ , where  $a$  is the difference between the bottom level of the tunnel and

that of the basin,  $r$  is the radius of the tunnel,  $X_s$  the arrival point of the jet axis to the bottom measured from the entrance section.

By solving the equations  $X_s = v_t \cdot t$  and  $Y_s = \frac{g}{2}t^2$ , the length of the first part of the upper basin  $X_s$  can be calculated.

Following the free fall of the jet, a three dimensional hydraulic jump develops which can be considered as the *second part of the upper basin*. The hydraulic jump is three dimensional because of the concentrated arrival with a width smaller than the width of the basin and it is expanded to the total width of the basin.

Applying the impulse-momentum theorem of fluid mechanics for the hydraulic jump, taking  $a$  as the starting depth  $h_1$  for the total width  $B$

$$\frac{\gamma h_1^2}{2}B - \frac{\gamma h_2^2}{2}B = \rho Q(v_2 - v_1),$$

and taking  $v_2 = \frac{Q}{h_2 B}$ ,  $h_2$  can be calculated as the depth of the flow after the hydraulic jump for the total width of the basin, considering the energy loss as negligible in the third part of the basin following the hydraulic jump.

When the depths of the hydraulic jump are known, the length of the jump as the length of the second part of the upper basin  $L_2$  can be calculated. From among the several well known formulas the most commonly used one is the Smetana formula (which can be used also for the three dimensional jump with an acceptable accuracy):

$$L_2 = 6(h_2 - h_1).$$

The theoretical description of the *third part of the upper basin* has been reached after the literature survey of side or lateral weirs. This will be described in chapter 4.2. The known side weir theories have been developed for the solution of our problem. The suggested method is detailed in chapter 4.4.

The structure studied can be considered as a special lateral weir on the side of a channel end, so the total discharge flows over the side weir, there is no further flow in the channel.

All the velocity and level measurements have proved that for each design value of the discharge the flow over the weir crest can be considered as of homogeneous discharge distribution along the weir length, i.e.  $q(x) = \text{constant}$ . This is also beneficial from the point of view of dimensioning the lower basin.

#### 4.2. Side Weir Calculation Methods

Basic, commonly applied arrangements with typical surface curves for the different flow conditions are presented by PREIBLER–BOLLRICH [12].

HENDERSON [8] published the general description of longitudinal inflow and outflow along the weir and the related surface curves.

Similar overview and the surface curves are presented by NAUDASCHER [10] but also considering the water levels before the start of the side weir and after the end of it.

All the sources give the same deduction for the  $dy/dx$  water level change along the length  $x$  of the side weir, the lateral overflow  $q = \frac{dQ}{dx}$  and for the discharge  $Q$  flowing on in the channel after the end of the weir.

The relation among the hydraulic and geometric parameters of a rectangular channel and side weir can be given as:

$$\frac{dy}{dx} = -\frac{Qy}{gB^2y^3 - Q^2},$$

where  $y$  is the water depth at point  $x$  of the weir,  $B$  is the width of the channel.

The specific lateral overflow  $q = -\frac{dQ}{dx} = C_q\sqrt{2g}(y-w)^{3/2}$ , where  $C_q$  is the discharge factor,  $w$  is the constant height of the weir crest above the bottom of the channel.

From the specific energy content it can be determined that

$$Q = By\sqrt{2g(e-y)},$$

where  $e = y + \frac{v^2}{2g}$ .

Putting the last two equations into the previous one, we get

$$\frac{dy}{dx} = \frac{2C_q}{B} \frac{\sqrt{(e-y)(y-w)^3}}{(3y-2e)}.$$

De Marchi integrated this differential equation for the first time and he got the following result

$$\frac{x C_q}{B} = \frac{2e-3w}{e-w} \sqrt{\frac{e-y}{y-w}} - 3 \sin^{-1} \sqrt{\frac{e-y}{y-w}} + \text{const.}$$

In many cases during the practical application of the equation it is rather difficult to determine the boundary conditions. We do not have too much information about the discharge factor either. Although, the afore-mentioned authors have published some approximative formulas and values.

JAIN and FISHER [9] have published the numerical and experimental results of an arrangement which makes it possible to have constant specific discharge outflow over the side weir with the reduction of the channel width along the weir.

According to their deduction the specific discharge flowing over the side weir

$$q = -\frac{dQ}{dx} = \frac{2}{3}\mu\sqrt{2g}(y-w)^{3/2}.$$

In any section of the channel the discharge is given by the formula  $Q = By\sqrt{2g(e-y)}$  mentioned above.

The thickness of the overflowing jet is given by the equation:

$$\frac{dy}{dx} = \frac{2(e-y)}{\left[B_2 + (B_1 - B_2)\left(1 - \frac{x}{L}\right)\right]} \frac{2\mu}{\sqrt[3]{e-y}} \left[(y-w)^{\frac{3}{2}} - (B_1 - B_2)\frac{y}{L}\right].$$

From the conditions  $\frac{dQ}{dx} = \text{const.}$  and  $\frac{Q}{B} = \text{const.}$  taken as a goal  $Q = -\frac{Q_i - Q_0}{L}x + Q_i$ , and  $B = \frac{Q_0}{Q_i}B_1 + \left(B_1 - B_1\frac{Q_0}{Q_i}\right)\left(1 - \frac{x}{L}\right)$  is coming, where  $Q_i$  is the arriving discharge through the upstream section and  $Q_0$  is the leaving discharge through the downstream section of the channel.

The ratio for the bottom width change of the channel is

$$B_2 = \frac{Q_0}{Q_i}B_1.$$

These results of JAIN and FISCHER were demonstrated by experimental results, as well.

#### 4.3. Development of the Side Weir Calculation for the Double Stilling Basin System

The detailed analysis of our experimental results has proved that for each design discharge value the flow over the weir crest can be considered as a homogeneous discharge distribution along the weir length. Thus, for the development of the calculation method the theoretical solutions of the constant specific discharge side weir were also applied.

Special conditions of our solution in the third part of the upper basin are the following:

- $Q_0 = 0$ , in other words, there is no further flow in the 'channel' after the weir, because of the end wall of the basin.
- $w = f(x) = ax + b$ , in other words, the weir crest level is not constant, but linearly changing along the length  $x$  of the weir.
- $B = \text{constant}$ , i.e. the width of the channel (in our case the basin) is not changing,  $\frac{dB}{dx} = 0$ .

In the following deduction the approximations applied and proved in the theoretical modelling have also been used.

The energy loss in this part of the basin is neglected (HENDERSON [8]).

$$\frac{de}{dx} = S_0 - S_f = 0.$$

Starting from the basic equation of HENDERSON [8]

$$\frac{dy}{dx} = \frac{S_0 - S_f - \frac{Q}{gA^2} \frac{dQ}{dx}}{1 - Fr^2}$$

and considering the above mentioned condition

$$\frac{dy}{dx} = \frac{1}{1 - Fr^2} \left( -\frac{Q}{gA^2} \frac{dQ}{dx} \right)$$

is received.

Applying the signature  $\frac{1}{1 - Fr^2} = FR$  and using

$$q = -\frac{dQ}{dx} = \frac{2}{3} \mu \sqrt{2g} [y(x) - w(x)]^{3/2}$$

the following statements can be made:

The experimental results have shown that the difference  $y(x) - w(x)$  can be considered as constant, or even if the constant specific discharge  $q(x) = \text{const.}$  is caused by the effect of the downstream water level, in the side weir calculation  $y(x) - w(x) = \text{const.} = h$  can be considered.

In our case  $Q_0 = 0$ , thus  $Q(x) = Q_i - \frac{Q_i}{L}x = Q_i - qx$ .

Summarising all these

$$\begin{aligned} \frac{dy}{dx} &= FR \frac{Q(x)}{gB^2 y^2(x)} \frac{2}{3} \mu \sqrt{2g} h^{3/2}, \\ \frac{dy}{dx} &= FR \frac{Q_i - qx}{gB^2 y^2(x)} q \end{aligned}$$

can be obtained.

For easier calculation using  $K = \frac{FRq}{gB^2}$  the following form can be received:

$$\frac{dy}{dx} = \frac{K(Q_i - qx)}{y^2(x)}.$$

The general solution:

$$y = \sqrt[3]{3K \left( Q_i x - \frac{qx^2}{2} \right) + C_1}.$$

$C_1$  can be determined from  $y_1$  known at the place  $x = 0$

$$C_1 = y_1^3.$$

For the easier solution we have applied the  $K = \frac{1}{1 - Fr^2} q$  replacement which also contains a variable parameter along the weir i.e. the Froude number.

The computer program made for the calculation used a starting value  $Fr_1$  for the first  $dx_1$  length and after the calculation of  $y_2$ , applying the predictor corrector method (RÁTKY [13]), using a corrected average value of  $\frac{Fr_2 - Fr_1}{2}$  it recalculates the level change on  $dx_1$ .

The deviation of the velocity distribution from the homogeneous one is taken into consideration with the dispersion factor of kinetic energy (Coriolis factor).

The final result of this calculation is the surface curve of the upstream side of a constant specific discharge side weir parallel to the weir crest formed by the end wall of the channel, in our case the basin.

Nevertheless, this calculation, because of the replacement  $y(x) - w(x) = \text{const.} = h$ , does not take into consideration the slope of the weir crest. The calculation method is after all good, since the homogeneous distribution of the discharge is caused by the common effect of the downstream water level and the change of the discharge factor along the weir (caused by the slope of the weir crest).

#### 4.4. The Lower Basin

The flow in the lower basin depending on the downstream water depth can be considered as a drowned hydraulic jump without supercritical flow in the basin.

The downstream water level has a significant effect on the operation of the afore treated lateral weir. With the constant depth calculated for the design discharge the overflow along the weir crest, starting from the higher end, can be less and less considered as free overflow. According to our measurements the width of the free overflow was less than one fourth of the total width. Meanwhile, the difference between the upstream water level, whose calculation was described in the previous chapter, and the weir crest level, in other words the height  $h$  of the overflow is increasing compared to the weir height  $w$ , which is decreasing. This has significant effect on the discharge factor  $\mu$ .

For this partly submerged weir completing the Poleni formula with a submergence factor  $\sigma$  and considering the change of  $\mu$  as a function of  $h/w$ , it is possible to have homogeneous discharge distribution along the weir with sloped weir crest and changing  $h$ , at the same time.

Based on the upstream levels and the constant downstream level, the slope of the weir crest can be calculated.

Changes of the discharge factor  $\mu$  can be calculated e.g. by the following formula:

$$\mu = 0.61 + 0.08 \frac{h}{w} \quad (\text{NAUDASCHER [10]}).$$

For the  $\sigma$  factor tables and curves are available, for our calculations we have used the curve of PREIßLER–BOLLRICH [12].

Other questions regarding the dimensioning of the lower basin are not detailed here.

## 5. Summary

Comparing the calculation and measurement results for a structure with the most critical  $90^\circ$  breaking angle has verified the theoretical model.

*The first part of the upper basin:*

Given data for the calculation:

- ✓ Diameter of the tunnel exit:  $d = 7$  m
- ✓ Bottom of the tunnel exit above the bottom of the upper basin:  $a = 4.7$  m
- ✓ Discharge  $Q = 810$  m<sup>3</sup>/s, from which the velocity in the tunnel

$$v_t = \frac{Q}{A} = \frac{Q}{\frac{d^2\pi}{4}} = 21.05 \text{ m/s.}$$

According to the calculations given in Chapter 4.1  $v_g = \sqrt{2g4.7} = 9.6$  m/s and  $v_l = \sqrt{21.05^2 + 9.6^2} = 23.14$  m/s, which value shows rather good conformity with the measured value 22.84 m/s in the model (23.75 m/s in the Duhok model).

The length calculated for the first part of the upper basin is:  $L_1 = 26.89$  m.

*The second part of the upper basin:*

Starting from  $h_1 = 5$  m,  $h_2 = 10.1$  m can be calculated. With the application of the Smetana formula the length of the hydraulic jump  $L_2 = 30.6$  m is calculated.

Considering the fact that  $h_2$  was calculated from the ratio of the velocity and the cross sectional area, but  $h_1$ , because of the hydrostatic pressure distribution was not only the depth of the fluid body moving with the velocity  $v_1$ , it can be seen that the hydraulic jump will be really longer. The three dimensional hydraulic jump's smaller starting width is also justifying a longer length consideration compared to the calculated value ( $L_1 + L_2 \cong 57.5$  m). In our model the length from the beginning of the upper basin till the starting point of the lateral weir was 65 m.

Table 1.

$x, m$	$Q, m^3/s$	$y, m$	$v, m/s$	$Fr, -$	$e, m$
0	810	10.00	8.10	0.6688	14.35
1	792	10.64	7.44	0.5302	14.29
2	774	10.98	7.05	0.4610	14.24
3	756	11.24	6.73	0.4108	14.19
4	738	11.44	6.45	0.3707	14.14
5	720	11.62	6.20	0.3372	14.10
6	702	11.77	5.96	0.3082	14.05
7	684	11.90	5.75	0.2827	14.01
8	666	12.03	5.54	0.2600	13.97
9	648	12.14	5.34	0.2395	13.94
10	630	12.24	5.15	0.2208	13.90
11	612	12.33	4.96	0.2037	13.87
12	594	12.41	4.79	0.1881	13.84
13	576	12.49	4.61	0.1735	13.81
14	558	12.56	4.44	0.1601	13.78
15	540	12.63	4.28	0.1476	13.75
16	522	12.69	4.11	0.1359	13.72
17	504	12.75	3.95	0.1250	13.69
18	486	12.80	3.80	0.1148	13.67
19	468	12.85	3.64	0.1053	13.64
20	450	12.89	3.49	0.0963	13.62
21	432	12.93	3.34	0.0879	13.59
22	414	12.97	3.19	0.0801	13.57
23	396	13.01	3.04	0.0727	13.55
24	378	13.04	2.90	0.0657	13.53
25	360	13.07	2.76	0.0592	13.51
26	342	13.09	2.61	0.0531	13.48
27	324	13.12	2.47	0.0474	13.46
28	306	13.14	2.33	0.0421	13.45
29	288	13.16	2.19	0.0371	13.43
30	270	13.17	2.05	0.0325	13.41
31	252	13.19	1.91	0.0282	13.39
32	234	13.20	1.77	0.0243	13.37
33	216	13.21	1.64	0.0206	13.36
34	198	13.22	1.50	0.0173	13.34
35	180	13.22	1.36	0.0143	13.32
36	162	13.23	1.22	0.0116	13.31
37	144	13.23	1.09	0.0091	13.29
38	126	13.23	0.95	0.0070	13.28
39	108	13.23	0.82	0.0051	13.26
40	90	13.22	0.68	0.0036	13.25
41	72	13.22	0.54	0.0023	13.23
42	54	13.21	0.41	0.0013	13.22
43	36	13.20	0.27	0.0006	13.21
44	18	13.19	0.14	0.0001	13.19
45	0	13.18	0.00	0.0000	13.18

Table 2.

$x, m$	$y', m$	$q, m^2/s$
1	9.09	19.6
2	9.19	19.7
3	9.28	19.8
4	9.37	19.9
5	9.46	20.0
6	9.56	20.0
7	9.65	20.0
8	9.74	20.0
9	9.84	20.0
10	9.93	20.0
11	10.02	20.0
12	10.11	19.9
13	10.21	19.9
14	10.30	19.8
15	10.39	19.7
16	10.49	19.6
17	10.58	19.5
18	10.67	19.5
19	10.77	19.4
20	10.86	19.3
21	10.95	19.2
22	11.04	19.1
23	11.14	19.0
24	11.23	18.9
25	11.32	18.7
26	11.42	18.5
27	11.51	18.4
28	11.60	18.2
29	11.69	18.1
30	11.79	17.9
31	11.88	17.7
32	11.97	17.6
33	12.07	17.4
34	12.16	17.0
35	12.25	16.7
36	12.34	16.4
37	12.44	16.0
38	12.53	15.7
39	12.62	15.4
40	12.72	15.1
41	12.81	14.7
42	12.90	14.4
43	12.99	14.1
44	13.09	13.8
45	13.18	13.5
$\Sigma$		817.0

*The third part of the upper basin:*

The model tests have proved that the water level along the side wall opposite to the side weir is slightly elevating. The velocity distributions described in the cross sections have shown that the discharge transporting velocity is significantly bigger than the mean velocity and the transporting width is smaller than the basin's total width.

Thus the calculation described in Chapter 4 should be made for a narrower active zone. This active zone is the discharge transporting zone of the 810 m<sup>3</sup>/s discharge. The width of this active zone can be calculated by the formula

$$Q = \int v_i \, dA \cong \sum v_i \, \Delta A$$

until we get the really transported discharge. The width in our case is 10–11 m. Also the water level is elevated from 10–11 m to 13 m which was also measured in the model. The negligibility of the specific energy loss has also been proved while the velocity along the longitudinal axis and the Froude number is decreasing to 0. The calculation results are shown in *Table 1*.

Concerning the excentricity of the jet entrance to the upper basin it can be stated that the excentricity forms the narrow active zone and keeps it beside the wall. Without excentricity the hydraulic jump might go through the side weir.

The discharge flowing over 1 m wide slices of the side weir has been calculated by a computer program taking into account the effect of the downstream level and the change of the discharge factor, as well.

The  $y$  level values of the former calculation have been slightly modified due to the significant drawdown towards the lower weir heights. These more accurate results are given in *Table 2*. The specific discharge values are showing approximately homogeneous distribution and the summarised discharge is 817 m<sup>3</sup>/s.

It can be stated that the double impact of the downstream water level and the change of the discharge factor  $\mu$  along the weir can result in approximately homogeneous discharge distribution. Thus the height and slope of the weir crest can be designed for the specific conditions.

## References

- [1] HASZPRA, O., Törtengelyű energiatorő medencerendszer alaprajzi és szerkezeti kialakítása. Összefoglaló jelentés (240.718/82). BME Vízépítési Tanszék, Budapest, 1982.
- [2] HASZPRA, O., Final Report I. on the Hydraulic Model Tests of the Duhok Dam. Project for the State Organization for Dams, Republic of Iraq. Budapest Technical University, Budapest, 1982.
- [3] HASZPRA, O.–KALINA, E.–PAPP, G., A 70 m High Morning Glory Spillway and its Broken-Axis Stilling Basin System. *International Conference on the Hydraulic Modelling of Civil Engineering Structures*, (B2), Coventry, England, 1982.
- [4] HASZPRA, O., Néhány hidraulikai probléma a vízépítésben. Székfoglalók 1999. Magyar Tudományos Akadémia, Budapest, 2000.

- [5] HASZPRA, O., Modelkperimentoj pri hidroteknikaj objektumoj de montara akvorezervejo. *Scienca Revuo* nro 50/4, 1999.
- [6] HAYDE, L., Energy Dissipation of a Water Jet in Broken-Axis Stilling Basin Systems (Diploma work). Technical University of Budapest, Department of Hydraulic Engineering, Budapest, 1982.
- [7] HAYDE, L., Törttengelyű energiátörő medencerendszerek hidraulikai vizsgálata. Egyetemi doktori értekezés. Budapesti Műszaki Egyetem. Budapest, 1995.
- [8] HENDERSON, F. M., *Open Channel Flow*. Macmillan Publishing Co., Inc. New York, 1966.
- [9] JAIN, S. C.–FISCHER, E. E., Uniform Flow over Skew Side-Weir. *Journal of the Irrigation and Drainage Division, ASCE* 108 (1982), No. IR2.
- [10] NAUDASCHER, E., *Hydraulik der Gerinne und Gerinnebauwerke*. Springer-Verlag, Wien, New York, 1992.
- [11] PAPP, G., Törttengelyű energiátörő medencerendszer kismintavizsgálata. *Hidrológiai Közlemény*, **73** (1993), No. 5.
- [12] PREIBLER, G.–BOLLRICH, G., *Technische Hydromechanik*, Band 1. VEB Verlag für Bauwesen, Berlin, 1985.
- [13] RÁTKY, I., *Hidraulika III. (Numerikus módszerek alkalmazása a hidraulikában)*. Tankönyvkiadó, Budapest, 1989.